Fuel 230 (2018) 474–482

Contents lists available at ScienceDirect

Fuel

journal homepage: www.elsevier.com/locate/fuel

Full Length Article

Fuel property effects on low-speed pre-ignition☆

Gurneesh S. Jatana, Derek A. Splitter*, Brian Kaul, James P. Szybist

Fuels, Engines, and Emissions Research Center, Oak Ridge National Laboratory, National Transportation Research Center, 2360 Cherahala Blvd, Knoxville, TN 37932, United States

GRAPHICAL ABSTRACT

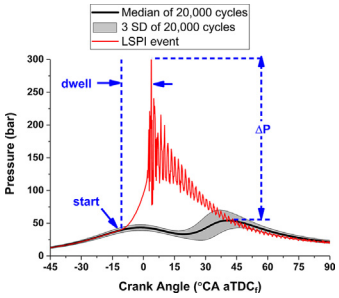

ARTICLE INFO

Keywords:
LSPI
Preignition
Superknock
Spark ignition
Fuel effects

ABSTRACT

This work explores the dependence of fuel distillation and flame speed on low-speed pre-ignition (LSPI). Findings are based on cylinder pressure analysis, as well as the number count, clustering, intensity, duration, and onset crank angle of LSPI events. Four fuels were used, with three of the fuels being blends with gasoline, and the fourth being neat gasoline. The blended fuels consisted of single molecules of different molecular types: a ketone (cyclopentanone), an alcohol (2-methyl-1-butanol), and an aromatic (ethylbenzene). All three pure molecules have RON values within ± 2 and boiling points within ± 5 °C. These fuels were blended with gasoline to a 25% mass fraction and were used to run the engine at identical LSPI prone operating conditions. The findings highlight that fuels with similar boiling properties and octane numbers can exhibit similar LSPI number counts, but with vastly different LSPI magnitudes and intensities. Moreover, the results highlight fundamental fuel properties such as flame speed are critical to characterizing the LSPI propensity and behavior of the fuel.

1. Introduction

As previously stated in [1], the US Department of Energy Co-Optimization of Fuels and Engines ("Co-Optima") initiative aims to foster the co-development of advanced fuels and engines for higher efficiency and lower emissions. A guiding principle of Co-Optima is the central fuel properties hypothesis (CFPH), which states that fuel properties provide an indication of the performance and emissions of the fuel, regardless of the fuel's chemical composition. CFPH is important because many of the fuel candidates being investigated in the Co-Optima initiative are bio-derived compounds with oxygen-containing functional groups typically not associated with commercial transportation fuels. The purpose of this investigation is to determine whether the fuel properties associated with low-speed preignition (LSPI), namely the

* Corresponding author.
E-mail address: splitterda@ornl.gov (D.A. Splitter).

https://doi.org/10.1016/j.fuel.2018.05.060
Received 15 February 2018; Received in revised form 1 May 2018; Accepted 11 May 2018

fuel boiling point and flame speed, are consistent with the CFPH.

Downsized and turbocharged spark-ignited engines are being increasingly used by engine manufacturers to both improve vehicle efficiency and reduce CO_2 emissions [1–3]. While these engines are greatly effective at improving fuel economy, their increased specific outputs make them more prone to damaging phenomena such as pre-ignition. Although pre-ignition is not a novel process or unique to downsized boosted engines [4], the high-load, low-speed operating conditions of these engines result in a particularly intense pre-ignition process which is typically referred to as LSPI. LSPI events often result in very strong knock event(s) that can cause significant damage to engine hardware, including catastrophic engine failure.

LSPI typically occurs during very-high-load operation at engine speeds around 2000 r/min or below wherein, the flame initiates before the spark is fired and leads to flame propagation at a significantly advanced combustion phasing. The increased pressure rise due to the advanced combustion phasing often causes violent end-gas knock or even 'superknock' for events that transition to developing detonation [5]. While the LSPI event and the resulting super-knock event are related, they are distinct phenomena, and not all LSPI cycles exhibit super-knock [6]. LSPI is apparently a stochastic phenomenon and, under appropriate operating conditions, will typically occur within every 10,000 cycles [7]. However, LSPI can also manifest as a cluster of many events that occur in an alternating pattern; wherein, every other cycle exhibits LSPI behavior. Additionally, though extremely rare, the occurrence of consecutive LSPI cycles has also been reported in literature [7].

Many studies have been reported in literature to better understand the factors responsible for LSPI onset and frequency. Zahdeh et al. [7] evaluated an engine's LSPI frequency over extensive operating condition sweeps and varying hardware configurations (e.g. injector targeting, piston top ring geometry, etc.). The results of these experiments illustrated the sensitivities of LSPI to different operating conditions and even provided some strategies to greatly reduce the frequency of pre-ignition events. These strategies included the use of a high volatility fuel, targeting the piston top rather than the cylinder liner with the fuel injection spray, and using multiple fuel injections.

However, the fundamental causes of LSPI still remain poorly understood, leading to a lack of firm consensus on the underlying mechanisms that promote LSPI. Zaccardi [8] describes many potential causes of LSPI such as auto-ignition in the gaseous phase and the ignition of fuel-air mixture due to either liquid droplets or solid particles. Furthermore, the presence of favorable thermodynamic conditions was observed to be necessary for all discussed mechanisms. Other researchers have also demonstrated the ability of appropriately-sized solid particulates, such as large soot particles or flaking deposits, in initiating LSPI events [9–11]. Although deposits or soot cinders are possible sources of LSPI, Gupta et al. [12] showed that these sources are highly improbable to persist over multiple cycles and thus are improbable as source for clustered LSPI events. Researchers have shown fuel/lubricant droplets to be a much more probable primary ignition source [7,13], and a significant amount of recent LSPI research has focused on understanding the effects of fuel [14–18] and lubricant [19–26] properties, as well as the interaction of fuel sprays and lubricating oil in the top crevice region [7,27,28]. Piston ring motion [7] and turbulence variations [29] have also been proposed as possible transport-related causes of the apparently stochastic nature of LSPI.

Physical properties, such as boiling point, have been shown to have an impact on the LSPI behavior of a fuel [17]. Fuels with higher boiling point have a higher probability of wetting the cylinder wall and mixing with the lubrication oil in the crevice regions. Some research has identified fuel with high aromatic content as being particularly prone to such processes [16]. This lubricant-fuel mixture, when ejected into the combustion chamber, can act as a source of ignition and cause LSPI.

In addition to the physical properties, chemical properties of a fuel can also play a role in causing LSPI. In literature, some efforts have been made to consider the pre-ignition from a chemical kinetics perspective, and to distinguish between deflagration and detonation in super-knock events [5]. Kalghatgi et al. [30,31] evaluated the formation of propagating flames from pre-ignition hotspots (which could be particles, fuel/oil droplets, etc.) and the severity of any resulting super-knock events based on analysis of ignition delays of surrogate fuels. Rudloff et al. [32] expanded upon this work and developed an analysis method, with a more detailed fuel chemistry rather than just surrogates, to characterize the transition of deflagration to detonation during the super-knock events. Lecoq et al. [33] developed a large eddy simulation model with integrated chemical-kinetics-based autoignition and simulated the formation of a flame front from a hotspot. Splitter et al. [34] explored the dependence of LSPI on fuel ignition delay, and specifically highlighted that the bulk gas thermodynamics and local high ignition delay gradient at highly boosted conditions are probable drivers of LSPI event magnitude and sensitivity. Kalghatgi et al. [35], recently explored the effects of stochastically-driven factors, such as pressure at knock onset and gradient of temperature with distance in the hotspots, on LSPI driven superknock events. Superknock was defined as a very high intensity knock which is a manifestation of developing detonation and is caused when the autoignition wave starts to couple with and amplify the pressure wave. It was found that while LSPI is necessary for superknock to occur, LSPI does not guarantee the onset of superknock. Furthermore, it was concluded that, all else being equal, higher flame speeds increase LSPI probability, and higher RON has no impact on the probability of LSPI but does reduce superknock probability.

As these previous studies highlight, there has been significant recent work to understand the processes governing LSPI; however, a gap still exists in the understanding of the impact of fuel properties, both physical and chemical, on LSPI behavior. The present study aims to provide more clarity on the relationship between fuel properties and LSPI; with fuel properties such as distillation and flame speed being specifically studied. Three molecules with similar RON (within ± 2) and boiling points (within ± 5 °C) were blended to 25% mass fraction with gasoline and tested at matched engine operating conditions that were conducive for promoting LSPI. Additionally, the LSPI behavior of 100% gasoline was also studied as the baseline case. The three molecules included a ketone (cyclopentanone), an alcohol (2-methyl-1-butanol), and an aromatic (ethylbenzene). The findings of this study highlight that fuels with similar boiling properties and octane numbers can exhibit similar LSPI number counts, but with vastly different LSPI magnitudes and intensities. Moreover, the results also highlight that, in addition to physical fuel properties such as boiling point, chemical fuel properties such as flame speed are also critical to the LSPI propensity and behavior of a given fuel.

2. Methodology

2.1. Experimental Facility

The engine used in this study is based on a 1.6 L Ford Ecoboost engine equipped with the production center-mounted direct injection fueling system. Engine geometry details are presented in Table 1.

The engine was converted to a single-cylinder engine by disabling cylinders 2, 3 and 4, where cylinder 1 is closest to the crank snout and cylinder 4 is closest to the flywheel. The three cylinders (Cylinders 2–4)

Table 1
Engine geometry.

Bore × Stroke (mm)	79.0 × 81.3
Connecting rod length (mm)	133
Wrist pin offset towards expansion stroke (mm)	0.8
Compression ratio	10.1:1
Fuel injection system	Direct injection, center-mounted production injector

were disabled by drilling holes in the pistons to prevent any compression work. Additionally, the camshaft lobes for these cylinders were also ground up to prevent the operation of valves [34]. The combustion chamber geometry and camshaft profiles on cylinder #1 were unchanged from the stock configuration. The engine was operated using standalone laboratory fueling and air handling systems. A pneumatically-actuated, positive displacement pump was utilized in conjunction with an electronic pressure regulator to maintain the fuel rail pressure at 150 bar throughout the study. Fuel flow to the engine was measured with a Coriolis-based fuel flow meter, and the start of fuel injection timing was commanded during the intake stroke at 300° CA $bTDC_f$ for all cases. Pressurized and dried facility air having less than 5% relative humidity was metered to the engine using an electronically-controlled mass air flow controller. Surge tanks were placed upstream of the intake as well as downstream of the exhaust to dampen the pressure oscillations associated with single-cylinder operation. The intake manifold gas temperature was maintained at 35 °C using an electrical heater that was placed upstream of the intake surge tank. An electronically-controlled valve, placed after the exhaust surge tank was used to maintain pressure differential across the engine, simulating realistic turbocharger boundary conditions. The engine was operated with a flipped pumping loop to simulate real engine conditions at high load, wherein, the intake manifold pressure was nominally 25 kPa higher than the exhaust manifold pressure. Furthermore, the coolant temperature was regulated to 65 °C to reduce fuel-liner vaporization rates and promote fuel retention in the top ring zone. Cylinder pressure was measured using a reinforced-diaphragm, flush-mounted piezoelectric pressure transducer (Kistler 6052c), which was also equipped with a flame arrestor.

Spark timing was adjusted as-needed to nominally maintain the desired crank angle of 50 percent mass fraction burned (CA50) combustion phasing at 38° $aTDC_f$, and spark dwell was held constant at 1.8 ms with a stock four wire ignition coil from a GM LNF engine. To prevent hot-spot run-away at high-load, a spark plug with 2 heat ranges colder than the production engine's plug was used. The corresponding colder spark plug was identified through cross-referencing current production spark plugs with the same thread and reach as the OEM spark plug, and a Denso Iridium HP ITV24 spark plug was identified as being compatible. Note the Denso spark plug is a 25 mm reach where the production spark plug is a 26.5 mm reach, and the 1.5 mm shorter reach of the Denso spark plug resulted in flush mounting of the spark plug to the combustion chamber while the stock 26.5 mm reach protruded into the combustion chamber approximately 1.5 mm.

As shown in Fig. 1, the factory-equipped, center-mount GDI injector is not mounted azimuthally symmetric due to the presence of the spark plug. Therefore, in stock orientation, the 6-hole spray pattern is biased towards the spark plug and away from the cylinder wall, potentially minimizing wall wetting. It has been previously shown that wall wetting can not only increase LSPI clustering tendency, but also significantly increase the LSPI event severity [34]. Therefore, to aid in increasing the probability of LSPI, the GDI injector was rotated 45° about its centerline to increase wall impingement by directing some of the fuel spray towards the wall. Fig. 1 also depicts this rotated injector orientation.

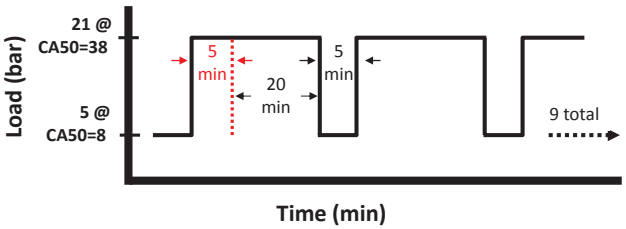

Fig. 2. Automated engine operating cycle.

The engine was controlled through a custom DRIVVEN-based engine controller, with automatic engine controls developed at ORNL using a calibration based on manual engine mapping. The controller used a mass-airflow-based PID control referencing tabular engine maps for fully automatic control of fuel, air, spark timing, and camshaft phasing. All measurements presented in this study were acquired in automated operation using time-varying load square-wave segments at 2000 r/min, and two such square waves are illustrated in Fig. 2. Each segment consisted of 5 min of operation at low-load (5 bar IMEPg), followed by 25 min of high-load (21 bar IMEPg) operation. The first 5 min of each 25-min high-load segment were thermally transient in boundary conditions and were discarded from the analysis such that only the last 20 min of data (20,000 cycles) of each high-load segment were used for the study of LSPI behavior. Finally, nine such consecutive low-high-low load square wave segments were run for each fuel mixture to ensure sufficient LSPI event count for consistent statistical analysis. Fresh engine oil (commercially available 5w-20 Mobil 1) was used for each fuel mixture.

2.2. Lubricant

All experiments were performed with commercially obtained Mobil 1 5W-20 lubricant. Independent lubricant analyses of this API service SN lubricant are listed in Table 2. After each of the four fuel mixtures, the engine was triple-flushed with fresh Mobil 1 lubricant and the engine oil was allowed to drain overnight after which fresh lubricant was used to continue testing.

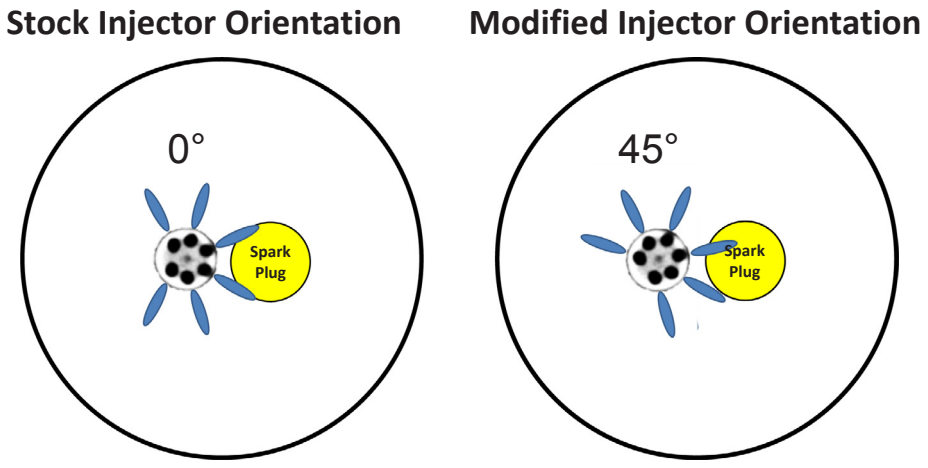

Fig. 1. Top view cartoon of GDI and spark plug orienting, stock left, modified right.

Table 2
Lubricant properties.

Silicon (ppm)	3
Boron (ppm)	93
Molybdenum (ppm)	76
Phosphorus (ppm)	703
Zinc (ppm)	803
Sodium (ppm)	0
Calcium (ppm)	1157
Magnesium (ppm)	411
Tungsten (ppm)	0
Viscosity at 100 °C (cSt)	8.9
Viscosity at 40 °C (cSt)	47.6
Viscosity Index	171
Total Base Number	7.01

2.3. Fuel properties

Premium-grade Tier II E0 certification fuel, acquired from Haltermann products (product code HFO437) was used as the baseline and blendstock for this study (hereby referred to as EEE). The baseline fuel was neat EEE, which was also used as a blend stock for blending with three secondary fuel components: Ethylbenzene, 2-Methyl-1-Butanol, and Cyclopentanone. The neat component molecular structure, RON, boiling point, and heat of vaporization (HoV) of these fuels are highlighted in Table 3, wherein, the HoV was determined from NIST data [36].

For this study, each of the neat molecules from Table 3 was mixed with EEE for a 25% by mass mixture. The three mixtures will be hereafter referred to as EB25, 2MB25, and CP25 for 25% by mass mixtures of Ethylbenzene, 2-Methyl-1-Butanol, and Cyclopentanone, respectively. Table 4 highlights fuel properties of EEE and the respective blends. These respective molecules were selected because they have different molecular structures but similar RON and neat boiling points (RON ± 2, boiling point ± 5 °C).

The complete range of fuel properties of the baseline and blended fuels are presented in Table 4. The three secondary fuels have very similar neat boiling points. However, the boiling points of the three secondary fuels are different when in a dilute solution with EEE gasoline. 2-Methyl-1-Butanol and Cyclopentanone, both of which have strong dipole moments [37], show a reduced boiling point in the dilute solution as compared to Ethylbenzene which has very weak dipolar moment [37]. Nevertheless, all three fuel components shift the baseline EEE distillation curve towards a higher boiling point.

2.4. LSPI Characterization

For the purpose of this study, a cycle was identified as LSPI if the peak recorded cylinder pressure and crank angle position of 5 percent mass fraction burned (CA05) were both more than 4 standard deviations greater than the median maximum cylinder pressure of all the cycles. The approach is similar to that described in detail by Mansfield et al. [16]. This method does not include events where pre-ignition occurred without leading to significantly higher in-cylinder pressure (i.e., non-knocking pre-ignition cycles), but effectively captures the potentially damaging events of interest, including both knock and superknock LSPI cycles. Each individual LSPI cycle was characterized using three parameters: LSPI event start location, LSPI dwell duration, and LSPI intensity. These three parameters are illustrated on a sample LSPI cycle in Fig. 3.

The LSPI event start location identifies the point of auto-ignition in crank-angle space and was defined as the first crank angle wherein the cylinder pressure trace of the LSPI event was observed to be more than 4 standard deviations greater than the median cylinder pressure trace. LSPI dwell duration characterized the time (in crank angles) required to achieve maximum pressure after pre-ignition has started, and LSPI intensity quantifies the increase in maximum cylinder pressure relative to the maximum pressure of the median trace. In addition to these three

Table 4
Fuel properties of neat Haltermann EEE premium grade fuel and 25% by mass fuel blends.

	EEE	CP25	2 MB25	EB25
Blended molecule	–	cyclopentanone	2-methyl-1-butanol	ethylbenzene
% of blended molecule in EEE by mass	–	25	25	25
% of blended molecule in EEE by volume	–	20	23	22
% o fblended molecule in EEE by mole	–	31	30	26
RON (ASTM D2699)	96.3	101.3	97.2	101
MON (ASTM D2700)	88.8	89.8	88.2	90.2
S (RON – MON)	7.5	11.5	9	10.8
IBP (°F) (ASTM D86)	87	87	89	90
T5 (°F) (ASTM D86)	114	111	119	118
T10 (°F) (ASTM D86)	127	131	136	138
T20 (°F) (ASTM D86)	148	162	168	170
T30 (°F) (ASTM D86)	171	195	200	204
T40 (°F) (ASTM D86)	200	221	221	230
T50 (°F) (ASTM D86)	220	232	230	242
T60 (°F) (ASTM D86)	231	240	236	251
T70 (°F) (ASTM D86)	241	248	244	261
T80 (°F) (ASTM D86)	257	258	255	274
T90 (°F) (ASTM D86)	315	275	275	298
T95 (°F) (ASTM D86)	340	278	332	321
FBP (°F) (ASTM D86)	411	279	394	388
C (wt%) (ASTM D5291)	86.58	82.88	82.07	87.67
H (wt%) (ASTM D5291)	13.42	12.36	13.38	12.33
O (wt%) (ASTM D4815)	0	4.76	4.55	0
LHV (MJ/kg) (ASTM D3338)	43	40.4	39.3	42.5
Aromatics (vol.%) (ASTM D1319)	28	–	–	–
Saturates (vol. %) (ASTM D1319)	71	–	–	–
Olefins (vol.%) (ASTM D1319)	1	–	–	–
RVP (psi) (ASTM D5191)	–	8.16	7.81	6.98
Specific Gravity (ASTM D4052)	0.744	0.7886	0.7613	0.7729

Table 3
Properties of interest for the three single molecule fuels [36].

Compound	Structure	Boiling point (°C)	RON	HoV (kJ/kg)	Molecular Weight (g/mol)	Density (kg/L)
ethylbenzene	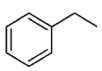	136	101	394	106	0.866
cyclopentanone	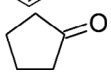	131	98	506	84	0.95
2-methyl-1-butanol	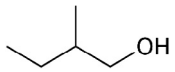	127.5	101	611	88	0.816

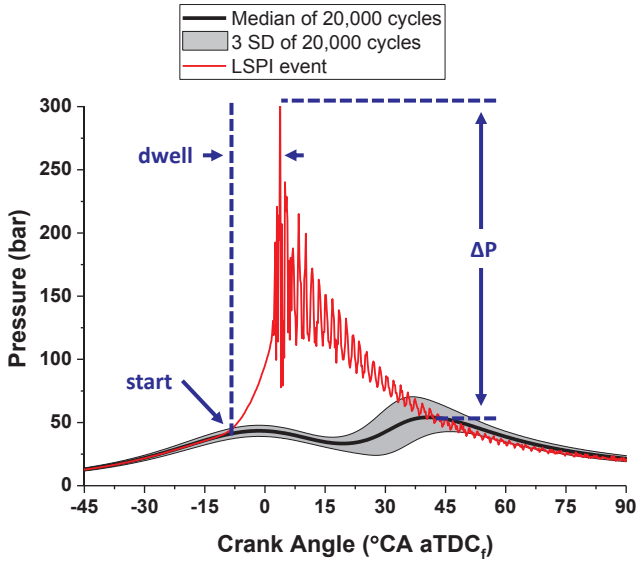

Fig. 3. LSPI event characterization parameters.

parameters, the total LSPI event number count and the cluster count of each fuel were also quantified for comparison. LSPI events were considered to be in a cluster if they were separated by no more than 4 consecutive non-LSPI cycles.

3. Results

As a control case, data was collected with EEE at both the beginning and end of testing, and similar LSPI behavior was observed in both EEE datasets. The complete order of testing EEE and the three fuel mixtures was EEE, EB25, 2MB25, CP25, and EEE. As shown in Fig. 4, compared to the baseline EEE fuel, all three blended fuels—25% ethylbenzene (EB25), 25% 2-methyl-1-butanol (2MB25), and 25% cyclopentanone (CP25)—nominally doubled the LSPI event count of the baseline EEE fuel (solid bars). The fraction of events occurring in clusters, on the other hand, was observed to be fairly consistent among the four fuels; wherein, a majority of LSPI events occurred in clusters for all four fuels, approximately 65–80% of the total events. However, as illustrated in Fig. 5, all the blended fuels exhibited an increased cluster count accompanied with a reduced event count per cluster. A possible reason for

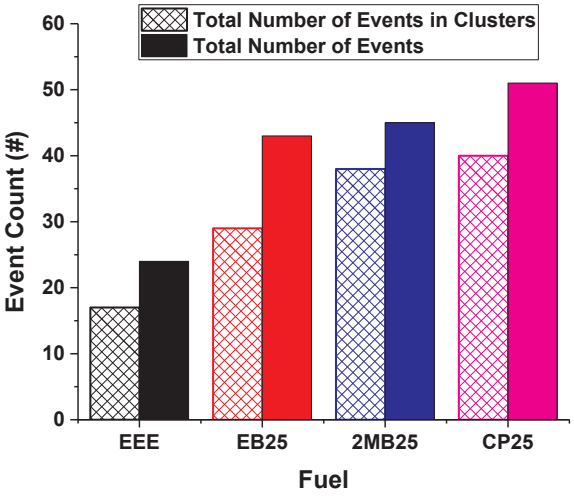

Fig. 4. LSPI count for the four tested fuel combinations. Solid bars depict the total number count of LSPI events, and cross-hatched bars represent the total number of those LSPI events that occur in clusters.

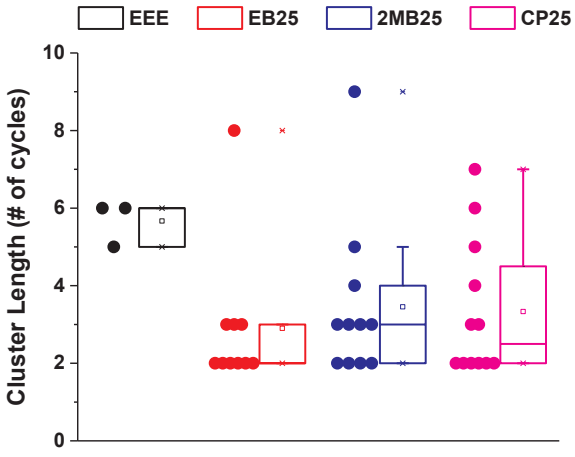

Fig. 5. LSPI cluster event length.

this behavior could be the higher rate of ignition source accumulation in the top ring zone with the blended fuels, which in turn would increase the frequency of cluster occurrence. Furthermore, increased cluster occurrence would reduce the residence time of the ignition source in the top ring zone, potentially reducing the extent of chemical or physical changes to the liquid accumulated in the top ring zone, and leading to fewer events per cluster.

Interestingly, in addition to increasing the total LSPI cluster count, all three blended fuels were also observed to advance the start of pre-ignition as compared to the baseline EEE gasoline, as shown in Fig. 6. While the effect of EB25 and 2MB25 on the start of LSPI events was minor, CP25 was observed to advance the mean LSPI phasing by more than 5° CA compared to EEE, equivalent to an entire data quartile (i.e., 25% faster). Additionally, CP25 also exhibited the largest spread in the observed LSPI start locations, with statically significant pressure rise of many LSPI cycles starting as early as 15° CA $bTDC_f$. The unique results of the CP25 indicate the presence of unique chemical and/or physical behaviors of the ketone at LSPI-prone conditions.

Fig. 7 shows the measured dwell times for the four fuel combinations. 2MB25 was observed to have the shortest mean dwell time (~11° CA), and therefore the fastest transition from start of pre-ignition to peak cylinder pressure. Additionally, most LSPI cycles observed with 2MB25 had similar dwell times, as indicated by the relatively short interquartile range (IQR) of 5° CA. EB25, on the other hand, exhibited the slowest transition from start of pre-ignition to peak cylinder pressure, as the mean dwell time of ~20° CA for the EB25 LSPI cycles was the longest among the four fuel mixtures studied here. Furthermore, as

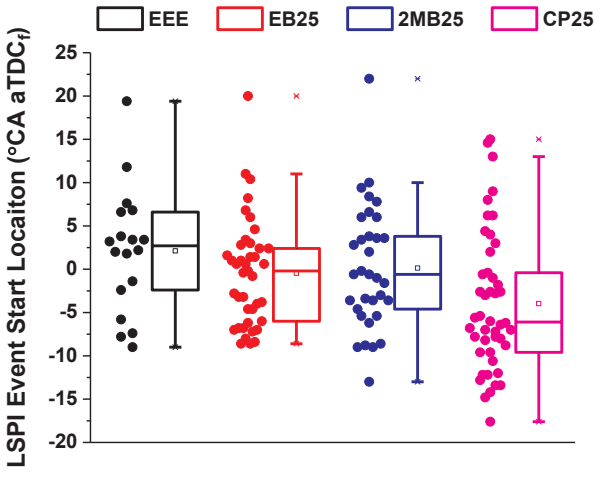

Fig. 6. The effect of different fuels on LSPI event start location.

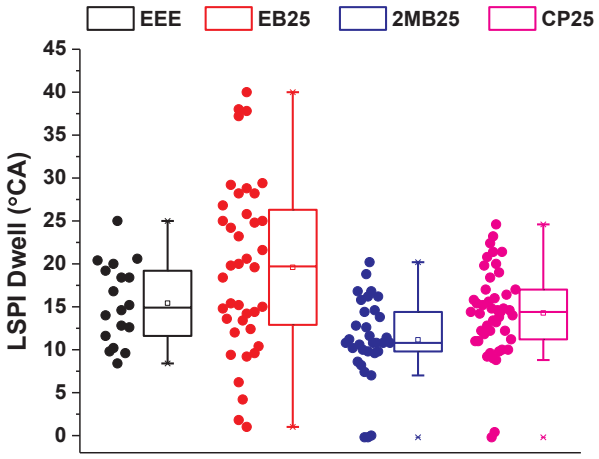

Fig. 7. Impact of various fuels on LSPI dwell.

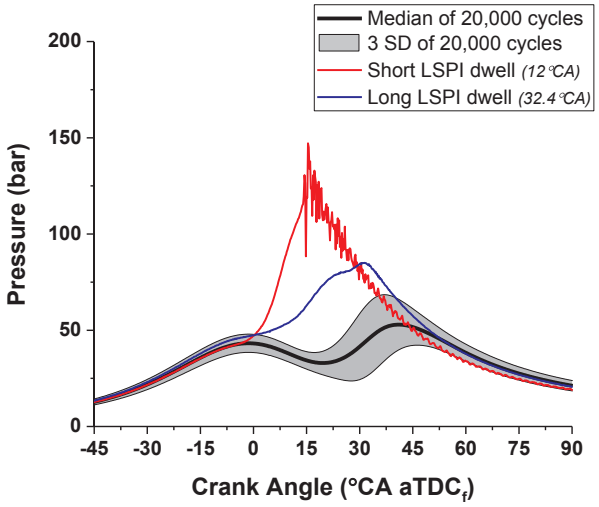

Fig. 8. Effect of LSPI dwell times on knocking behavior. LSPI cycles with long dwell time exhibit negligible end-gas knock. Sample long and short dwell time LSPI cycles are plotted here for operation with EB25.

also shown in Fig. 7, the spread of the observed dwell times for all EB25 LSPI cycles was also the largest, with the measured IQR of EB25 LSPI cycles being around twice the next highest IQR (observed for EEE). Many of the long-dwell LSPI cycles with EB25 were observed to have a slow enough burn rate that they never transitioned into superknock, as highlighted in Fig. 8. CP25 was observed to have a similar LSPI dwell behavior as that of the baseline EEE fuel, with both fuels having similar mean dwell times. However, CP25 did exhibit a slightly shorter IQR of dwell times compared to EEE, indicating more bias of CP25 towards slightly shorter dwell times. Lastly, it should be noted that the zero dwell times observed for the three secondary fuel mixtures were a measurement peculiarity created by the superknock events that either saturated the transducer charge amplifier or caused it to reset.

The LSPI dwell time effects in Figs. 7 and 8 reinforce the heavy knock trends shown in Fig. 9, wherein the mean LSPI intensity (ΔP) was observed to generally follow the mean measured LSPI dwell time for each fuel mixture. For example, the 2MB25 mixture, which was observed to have the shortest dwell, also exhibits the strongest mean LSPI intensity, with several LSPI events reaching cylinder pressures in excess of 500 bar. The CP25 mixture also produced strong LSPI cycles, with the overall distribution being shifted towards stronger LSPI events as compared to the baseline EEE fuel. Some strong LSPI cycles were observed with EB25, however, many of the EB25 LSPI cycles were very mild in nature (ΔP < 100 bar) resulting in a smaller mean LSPI

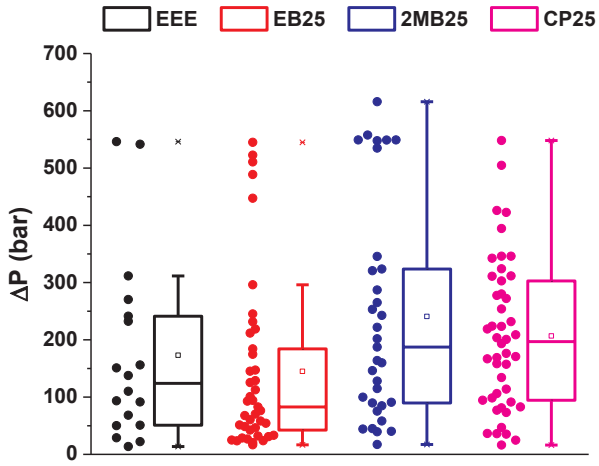

Fig. 9. LSPI intensity observed with various fuels.

intensity than the baseline EEE fuel. These very mild LSPI cycles of EB25 were observed to also have the longest dwell durations.

4. Discussion

The significantly increased LSPI number counts observed with the three blended fuels over the baseline EEE fuel could potentially be a result of a net increase in the fraction of heavy components in the fuel mixture. It is possible that the increased fuel distillation of the blended fuels could increase in-cylinder fuel-air stratification, where richer charge regions could exhibit reduced ignition delay [34], but the degree of this is beyond the current scope and at the operating conditions, is not thought to be significant. In a diluted solution, the polar Cyclopentanone and 2-Methyl-1-Butanol are expected to have a lower boiling point than the non-polar Ethylbenzene which is expected to maintain its neat boiling point. This is observed in the ASTM D86 distillation trends of the three 25% by mass mixtures, wherein, the T50-T80 region of EB25 is at a significantly higher temperature as compared to the distillation curves of CP25, 2MB25, and EEE (which exhibit similar behavior in this region). However, in spite of the differences in the distillation curves, the three blended fuel mixtures exhibit very similar LSPI number count, i.e., approximately two times greater than that of EEE. Moreover, despite exhibiting very similar distillation curves, CP25 and 2MB25 produced LSPI events that were observed to be very different in nature. Therefore, it is hypothesized that physical properties (such as boiling point) alone are not sufficient to predict LSPI behavior of a fuel mixture and that the chemical properties of the mixture components also play a crucial role.

As shown in Table 3, the calculated enthalpy of vaporization (HoV) of the three secondary fuels is very different, wherein Ethylbenzene has the lowest HoV, 2-methyl-1-butanol has the highest, and cyclopentanone is almost directly in between. The boiling point of the three secondary fuels, although similar, does differ slightly (8.5 °C maximum difference); wherein Ethylbenzene has the highest boiling point, 2-methyl-1-butanol the lowest, and the boiling point of cyclopentanone is in between. Both higher HoV and boiling point should reduce the rate of in-cylinder fuel vaporization. Therefore, the similar LSPI event counts observed with the three secondary fuels in spite of their differences in HoV and boiling point could potentially be explained by the opposite trend in HoV and boiling point of the three fuels counteracting the individual effect of these properties. Therefore, the physical properties of fuel such as distillation and HoV can be hypothesized to affect total LSPI number count. This hypothesis agrees with the reports of increased LSPI event activity with reduced fuel volatility in the cited literature studies [13–17], wherein reduced fuel vaporization plays a dominant role in increasing LSPI event-causing ignition sources through

increased fuel-lubricant interaction and top-ring-zone liquid retention. This hypothesis is also supported by the reduction in LSPI event count with the more volatile EEE fuel. However, even though the total number LSPI events were similar between the blended fuels, a broad range of variation in LSPI intensity (ΔP), LSPI dwell, and LSPI starting point was observed between them. Therefore, in addition to a fuel's physical properties, it's kinetic behavior also directly affects the LSPI combustion process.

Although the blended fuels had similar physical fuel properties, the fundamental combustion behaviors of the neat components differed. For example, the unstretched laminar flame speeds between the neat fuels varies significantly. Work by Hu et al. [38] measured the unstretched laminar flame speeds of ethanol, cyclopentanone, and gasoline at 423 K and 1 bar pressure, showing that in a stoichiometric mixture the flame speed of cyclopentanone was nearly that of ethanol, approximately a 10% increase in flame speed relative to gasoline. Li et al. [39], reported unstretched flame speed measurements at a temperature of 393 K and 1 bar pressure, showing that the flame speed of 2-methyl-1-butanol was approximately 15% slower than ethanol and 15% faster than isooctane; they also reported flame speed measurements of 2-methyl-1-butanol at a higher temperature condition of 433 K 1 bar pressure. At this higher temperature condition, the upstretched laminar flame speed of 2-methyl-1-butanol was approximately 15% slower than cyclopentanone and 8% slower than the gasoline data obtained by Hu et al. [38], suggesting that 2-ethyl-1-butanol has a slower flame speed compared to cyclopentanone at similar conditions. The studies by Hu et al. [38] and Li et al. [39] were conducted at elevated temperatures of 423 K and 433 K, respectively, but at 1 bar pressure.

Flame speed measurements of ethylbenzene have also been reported in Johnston and Farrell [40] and Farrell et al. [41], at a further elevated temperature of 450 K and a higher pressure of 3.04 bar. Thus, the extensive datasets by Johnston and Farrell [40] and Farrell et al. [41] are not directly comparable to the data sets of Hu et al. [38] and Li et al. [39]. Farrell et al. [41] also reported data for ethanol and isooctane at their higher pressure and temperature condition. Using that as a framework, ethylbenzene exhibited an unstretched flame speed approximately 12% faster than isooctane and 19% slower than ethanol, a similar trend-wise result to the 2-methyl-1-butanol data reported by Hu et al. [38] at their lower temperature and pressure conditions. Thus, it is reasonable to estimate the flame speed of 2-methyl-1-butanol is slightly faster than ethylbenzene at matched conditions, with both fuels having slower unstretched laminar flame speeds relative to cyclopentanone.

The cited literature assesses the unstretched laminar flame speeds of the neat components tested in the present work; however, these studies do not measure flame speed of cyclopentanone, ethylbenzene, or 2-methyl-1-butanol in a mixture with gasoline. To estimate the unstretched laminar flame speeds of the fuels tested in the present work, the energy fraction mixing rules proposed by Sileghem et al. for alternative fuels [42] and primary reference fuels with toluene [43] are used. The molecular weight of gasoline was assumed to be 110 g/mol as estimated by Anderson et al. [44], and the flame speed of the gasoline used in the present work was identical to that reported by Hu et al. [38], ~71 cm/s at their tested condition. The unstretched laminar flame speeds of the blended fuels in this study were estimated at 423 K and 1 bar pressure using these assumptions and approximations as: ~63 cm/s for ethylbenzene, 71 cm/s for gasoline, 78 cm/s for cyclopentanone, and 66 cm/s for 2-methyl-1-butanol.

The estimated flame speed trends in Fig. 10 qualitatively agree with the LSPI starting location and dwell times reported earlier in this study, wherein CP25 has the fastest estimated flame speed and the earliest measured LSPI starting location, and EB25 had the slowest estimated flame speed and longest measured LSPI dwell times. The estimates of flame speed, which in this study are derived from literature data and analysis approaches, suggest that fuel flame speed could be an important factor in determining the statistically significant relative onset

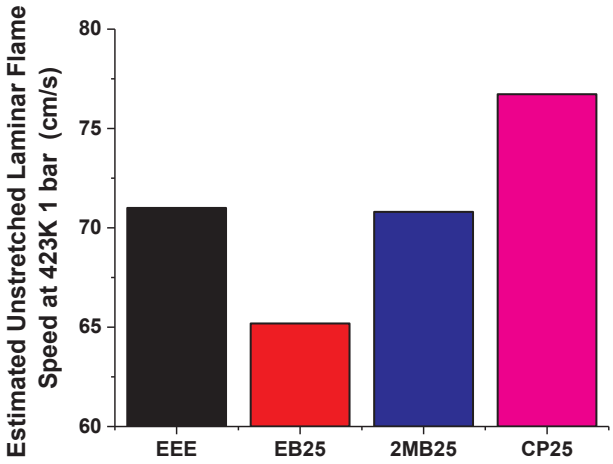

Fig. 10. Estimated unstretched laminar flame speeds of fuel mixtures at 423 K, 1 bar.

of LSPI events, as well as the corresponding statistically significant intensity of the LSPI events. This qualitatively agrees with the suggestion of Klaghatgi et al. [45] that flame thickness, which is highly dependent on flame speed, could be a contributing factor to a fuel's LSPI propensity.

The present work highlights that on average, the LSPI events of CP25 exhibited a much earlier start of combustion as opposed to baseline EEE or other fuels, in agreement with the hypothesis that flame speed affects LSPI behavior. 2MB25 had a similar starting location of LSPI events as that of EEE LSPI events, and also had a similar estimated flame speed to EEE, again suggesting agreement with the hypothesis that flame speed affects LSPI behavior. Lastly, the LSPI starting location of the EB25 fuel was similar to the EEE and 2MB25 fuels, but the LSPI dwell time of the EB25 fuel was significantly more variable with many LSPI events being as much as double in duration as compared to the longest LSPI events with the other fuels. Although the EB25 LSPI starting location results are not directly in agreement with the theory of flame speed affecting LSPI behavior, the increased LSPI dwell time of the EB25 fuel reduced the magnitude of many of the LSPI events, resulting in an overall reduced LSPI intensity even though the LSPI events with EB25 started at timings relatively similar to fuels with faster estimated flame speeds (EEE and 2MB25). Even with these qualitative agreements, some discrepancies exist in the estimated flame speeds and the observed LSPI behavior. For example, the flame speed of 2MB25 is similar to that of the baseline EEE gasoline, but 2MB25 also exhibited the lowest average LSPI dwell time of all fuels. These discrepancies could be explained by changes in fuel chemistry/kinetics at near top-dead-center in-cylinder temperatures and pressures, which will be significantly higher than the conditions used to estimate flame speeds in this study. As such, a comprehensive chemical kinetics modeling exercise could provide more clarity on the reasons for the observed LSPI behavior.

It should be noted that differences exist between concentrations in liquid and gas phase mixtures. The fuels selected in the present current work were blended on a mass basis, which mostly affects the molar concentrations of the liquid phase, and thus the present work was primarily designed to address liquid ejection from the top ring zone that is thought to be responsible for a LSPI ignition source. However, the current blended fuels are also in the gas phase, where the flame speed of the mixture is suggested to affect LSPI intensity. The molar concentrations of the EB25 blended fuel is quite different in the gas phase, where it has reduced molar concentration by approximately 5% on an absolute or 15% on a relative basis compared to the 2MB25 or CP25 fuels. However, from the gas phase perspective, the molar density of the fuel is not what correlates to flame speed; instead the energy fraction is

more appropriate. From this perspective, EB25 has the highest energy fraction even though it has the lowest gas phase molar concentration. Unfortunately, with a common fuel blending basestock there is no direct method to independently hold the liquid molar and energy-based parameters constant while varying the composition, as there are a lot of composition-dependent properties. Since it was not possible to run each fuel four different ways within the scope of the study (i.e., mass fraction, volume fraction, mole fraction, and energy fraction), the authors have attempted to balance the conclusions as best as possible. Since the EB25 fuel had the highest energy fraction of the various fuel blends, the authors conclude that the lower LSPI intensity is a real effect occurring from the gas phase fuel properties, while the source term is relatively consistent amongst the fuels and is attributed to liquid phase concentrations which were similar between the blended fuels.

5. Conclusions

The aim of this study was to further the understanding on the effect of fuel properties on LSPI. Three single component fuels, a ketone (cyclopentanone), an alcohol (2-methyl-1-butanol), and an aromatic (ethylbenzene), were mixed by 25% mass fraction in gasoline. Engine testing was then performed on a modern turbocharged and downsized direct injection spark ignited engine at conditions conducive for promoting LSPI, i.e. high load (21 bar BMEP at late combustion phasing, 38 °CA $aTDC_f$) at low engine speed (2000 r/min). The recorded in-cylinder pressure data was then processed to isolate the LSPI events, i.e. events that exhibited a 4-standard deviation in both increased peak cylinder pressure and earlier CA05. The identified LSPI events were further characterized as single events or clusters, as well as based on their start of pre-ignition, dwell, and intensity.

Compared to the baseline EEE fuel, all three fuel blends were observed to roughly double the amount of LSPI events, possibly due to the net increase of heavy components in the fuel caused by blending the three heavier fuels with gasoline. The three fuel components were also observed to have a similar total LSPI event count and similar LSPI clustering tendency in spite of having different distillation properties, as well as different boiling point and HoV of the neat secondary fuels therefore, illustrating the impact of physical properties of the fuel on LSPI behavior, wherein the offsetting impact of boiling point and HoV resulted in a net similar behavior for the three fuel blends. However, even though the three blends exhibited similar LSPI counts, distinct differences were observed in the characteristics of the LSPI events produced with the three fuels; therefore confirming the role of kinetic properties of the fuel, in addition to the physical properties, in determining it's LSPI behavior. The flame speed estimates of the four fuel combinations, derived from literature data and analysis approaches, qualitatively correlated with the LSPI behavior observed with each fuel. CP25 was estimated to have the highest flame speed and was observed on average to also have the earliest start of pre-ignition as well as one of the highest LSPI intensities among the four fuels. On the other hand, EB25 was calculated to have the lowest flame speeds and was observed to also have the lowest average LSPI intensity. While a more detailed chemical kinetics effort would improve the understanding of fuel kinetic effects on the LSPI behavior, the present global trends suggest that for a given fuel distillation curve and engine operating thermodynamic conditions, increased fuel laminar flame speed seems to increase LSPI event intensities, though it does not increase the propensity of a fuel to exhibit LSPI events. Finally, both physical and kinetic properties of the fuel play a significant role in shaping its LSPI behavior.

Acknowledgments

This research was conducted as part of the Co-Optimization of Fuels & Engines (Co-Optima) project sponsored by the U.S. Department of Energy (DOE) Office of Energy Efficiency and Renewable Energy (EERE), Bioenergy Technologies and Vehicle Technologies Offices. Co-Optima is a collaborative project of multiple National Laboratories initiated to simultaneously accelerate the introduction of affordable, scalable, and sustainable biofuels and high-efficiency, low-emission vehicle engines. A special thanks is due to program managers Kevin Stork, Gurpreet Singh, Leo Breton, and Mike Weismiller.

References

[1] Szybist James P, Splitter Derek A. Understanding chemistry-specific fuel differences at a constant RON in a boosted SI engine. Fuel 2018;217:370–81. http://dx.doi.org/10.1016/j.fuel.2017.12.100.
[2] Pawlowski A, Splitter D. SI Engine Trends: A Historical Analysis with Future Projections, SAE Technical Paper 2015-01-0972; 2015. doi:10.4271/2015-01-0972.
[3] Splitter D, Pawlowski A, Wagner R. A historical analysis of the co-evolution of gasoline octane number and spark-ignition engines. Front Mech Eng 2016;1(1). http://dx.doi.org/10.3389/fmech.2015.00016.
[4] Chapman EM, Costanzo VS. A literature review of abnormal ignition by fuel and lubricant derivatives. SAE Int J Engines 2016;9(1). http://dx.doi.org/10.4271/2015-01-1869.
[5] Wang Z, Qi Y, He X, Wang J, Shuai S, Law CK. Analysis of pre-ignition to super-knock: hotspot-induced deflagration to detonation. Fuel 2015;144:222–7. http://dx.doi.org/10.1016/j.fuel.2014.12.061.
[6] Wang Z, Liu H, Song T, Qi Y, He X, Shuai S, et al. Relationship between super-knock and pre-ignition. Int J Engine Res 2015 February;16(2):166–80. http://dx.doi.org/10.1177/1468087414530388.
[7] Zahdeh A, Rothenberger P, Nguyen W, Anbarasu M, Schmuck-Soldan S, Schaefer J, et al. Fundamental approach to investigate pre-ignition in boosted SI engines. SAE Int J Engines 2011;4(1):246–73. http://dx.doi.org/10.4271/2011-01-0340.
[8] Zaccardi JM, Escudie D. Overview of the main mechanisms triggering low-speed pre-ignition in spark-ignition engines. Int J Engine Res 2015;16(2):152–65. http://dx.doi.org/10.1177/1468087414530965.
[9] Haenel P, Seyfried P, Kleeberg H, Tomazic D. Systematic Approach to Analyze and Characterize Pre-Ignition Events in Turbocharged Direct-Injected Gasoline Engines, SAE Technical Paper 2011-01-0343; 2011. doi:10.4271/2011-01-0343.
[10] Wang Z, Qi Y, Liu H, Long Y, Wang JX. Experimental Study on Pre-Ignition and Super-Knock in Gasoline Engine Combustion with Carbon Particle at Elevated Temperatures and Pressures, SAE Technical Paper 2015-01-0752; 2015. doi:10.4271/2015-01-0752.
[11] Okada Y, Miyashita S, Izumi Y, Hayakawa Y. Study of low-speed pre-ignition in boosted spark ignition engine. SAE Int J Engines 2014;7(2):584–94. http://dx.doi.org/10.4271/2014-01-1218.
[12] Gupta A, Seeley R, Shao H, Remias J. Impact of particle characteristics and engine conditions on deposit-induced pre-ignition and superknock in turbocharged gasoline engines. SAE Int J Fuels Lubr 2017;10(3). http://dx.doi.org/10.4271/2017-01-9379.
[13] Dahnz C, Han KM, Spicher U, Magar M, Schießl R, Maas U. Investigations on pre-ignition in highly supercharged SI engines. SAE Int J Engines 2010;3(1):214–24. http://dx.doi.org/10.4271/2010-01-0355.
[14] Mansfield AB, Chapman E, Briscoe K. Effect of market variations in gasoline composition on aspects of stochastic pre-ignition. Fuel 2016;184:390–400. http://dx.doi.org/10.1016/j.fuel.2016.07.010.
[15] Amann M, Mehta D, Alger T. Engine operating condition and gasoline fuel composition effects on low-speed pre-ignition in high-performance spark-ignited gasoline engines. SAE Int J Fuels Lubr 2011;4(1):274–85. http://dx.doi.org/10.4271/2011-01-0342.
[16] Mansfield AB, Chapman E, Briscoe K. Impact of Fuel Octane Rating and Aromatic Content on Stochastic Pre-Ignition, SAE Technical Paper 2016-01-0721; 2016. doi:10.4271/2016-01-0721.
[17] Chapman E, Davis R, Studzinski W, Geng P. Fuel Octane and volatility effects on the stochastic pre-ignition behavior of a 2.0L gasoline turbocharged DI ENGINE. SAE Int J Fuels Lubr 2014;7(2). http://dx.doi.org/10.4271/2014-01-1226.
[18] Mansfield AB, Chapman E, Briscoe K. Effect of market variations in gasoline composition on aspects of stochastic pre-ignition. Fuel 2016;184:390–400. http://dx.doi.org/10.1016/j.fuel.2016.07.010.
[19] Welling O, Collings N, Williams J, Moss J. Impact of lubricant composition on low-speed pre-ignition, SAE Technical Paper 2014-01-1213, 2014. doi:10.4271/2014-01-1213.
[20] Welling O, Moss J, Williams J, Collings N. Measuring the impact of engine oils and fuels on low-speed pre-ignition in downsized engines. SAE Int J Fuels Lubr 2014;7(1). http://dx.doi.org/10.4271/2014-01-1219.
[21] Mayer M, Hofmann P, Geringer B, Williams J, Moss J, Kapus P. Influence of Different Oil Properties on Low-Speed Pre-Ignition in Turbocharged Direct Injection Spark Ignition Engines, SAE Technical Paper 2016-01-0718; 2016. doi:10.4271/2016-01-0718.
[22] Fletcher KA, Dingwell L, Yang K, Lam WY, Styer JP. Engine oil additive impacts on low speed pre-ignition. SAE Int J Fuels Lubr 2016;9(3). http://dx.doi.org/10.4271/2016-01-2277.
[23] Ritchie A, Boese D, Young AW. Controlling low-speed pre-ignition in modern automotive equipment part 3: identification of key additive component types and other lubricant composition effects on low-speed pre-ignition. SAE Int J Engines 2016;9(2). http://dx.doi.org/10.4271/2016-01-0717.
[24] Dingle S, Cairns A, Zhao H, Williams J, Williams O, Ali R. Lubricant Induced Pre-Ignition in an Optical SI Engine, SAE Technical Paper 2014-01-1222; 2014. doi:10.

4271/2014-01-1222.
[25] Qi Y, Xu Y, Wang Z, Wang J. The Effect of Oil Intrusion on Super Knock in Gasoline Engine, SAE Technical Paper 2014-01-1224; 2014. doi:10.4271/2014-01-1224.
[26] Whitby RD. Engine oils and low-speed pre-ignition. Tribol Lubric Technol 2015;71(9). http://dx.doi.org/10.3390/lubricants5020009.
[27] Dahnz C, Spicher U. Irregular combustion in supercharged spark ignition engines—pre-ignition and other phenomena. Int J Engine Res 2010;11(6):485–98. http://dx.doi.org/10.1243/14680874JER609.
[28] Amann M, Alger T, Westmoreland B, Rothmaier A. The effects of piston crevices and injection strategy on low-speed pre-ignition in boosted SI engines. SAE Int J Engines 2012;5(3). http://dx.doi.org/10.4271/2012-01-1148.
[29] Peters N, Kerschgens B, Paczko G. Super-knock prediction using a refined theory of turbulence. SAE Int J Engines 2013;6(2). http://dx.doi.org/10.4271/2013-01-1109.
[30] Kalghatgi GT, Bradley D, Andrae J, Harrison AJ. The nature of superknock and its origins in SI engines. Internal combustion engines: performance, fuel economy, and emissions Institution of Mechanical Engineers978-1843346074; 2009. p. 259–69.
[31] Khalghatgi GT, Bradley D. Pre-ignition and super-knock in turbo-charged spark-ignition engines. Int J Engine Res 2012;13(4):399–414. http://dx.doi.org/10.1177/1468087411431890.
[32] Rudloff J, Zaccardi J, Richard S, Anderlohr J. Analysis of pre-ignition in highly charged SI engines: emphasis on the auto-ignition mode. Proc Combust Inst 2013;34(2):2959–67. http://dx.doi.org/10.1016/j.proci.2012.05.005.
[33] Lecocq G, Richard S, Michel JB, Vervisch L. A new LES model coupling flame surface density and tabulated kinetics approaches to investigate knock and pre-ignition in piston engines. Proc Combust Inst 2011;33(2):3105–14. http://dx.doi.org/10.1016/j.proci.2010.07.022.
[34] Splitter D, Kaul B, Szybist J, Jatana G. Engine operating conditions and fuel properties on pre-spark heat release and SPI promotion in SI engines. SAE Int J Engines 2017;10(3):1036–50. http://dx.doi.org/10.4271/2017-01-0688.
[35] Kalghatgi G, Algunaibet I, Morganti K. On knock intensity and superknock in SI engines. SAE Int J Engines 2017;10(3):1051–63. http://dx.doi.org/10.4271/2017-01-0689.
[36] Stephenson Richard M, Stanislaw Malanowski. Handbook of the thermodynamics of organic compounds 1987. http://dx.doi.org/10.1007/978-94-009-3173-2.
[37] Haynes William M, Lide David R. CRC handbook of chemistry and physics: a ready-reference book of chemical and physical data Boca Raton: CRC Press978-1420090840; 2009.
[38] Hu S, Gao J, Gong C, Zhou Y, Bai XS, Li ZS, et al. Assessment of uncertainties of laminar flame speed of premixed flames as determined using a Bunsen burner at varying pressures. Appl Energy 2017. http://dx.doi.org/10.1016/j.apenergy.2017.09.083.
[39] Li Qianqian, Erjiang Hu, Cheng Yu, Huang Zuohua. Measurements of laminar flame speeds and flame instability analysis of 2-methyl-1-butanol–air mixtures. Fuel 2013;112:263–71. http://dx.doi.org/10.1016/j.fuel.2013.05.039.
[40] Johnston RJ, Farrell JT. Laminar burning velocities and Markstein lengths of aromatics at elevated temperature and pressure. Proc Combust Inst 2005;30(1):217–24. http://dx.doi.org/10.1016/j.proci.2004.08.075.
[41] Farrell JT., Johnston RJ, Androulakis IP. Molecular structure effects on laminar burning velocities at elevated temperature and pressure. SAE Technical Paper 2004-01-2936; 2004. doi:10.4271/2004-01-2936.
[42] Sileghem Louis, Vancoillie Jeroen, Demuynck Joachim, Galle Jonas, Verhelst Sebastian. Alternative fuels for spark-ignition engines: mixing rules for the laminar burning velocity of gasoline–alcohol blends. Energy Fuels 2012;26(8):4721–7. http://dx.doi.org/10.1021/ef300393h.
[43] Louis Sileghem, Alekseev VA, Vancoillie Jeroen, Van Geem KM, Nilsson EJK, Verhelst Sebastian, Konnov AA. Konnov, Laminar burning velocity of gasoline and the gasoline surrogate components iso-octane, n-heptane and toluene. Fuel 2013;112:355–65. http://dx.doi.org/10.1016/j.fuel.2013.05.049.
[44] Anderson JE, Kramer U, Mueller SA, Wallington TJ. Octane numbers of ethanol − and methanol − gasoline blends estimated from molar concentrations. Energy Fuels 2010;24(12):6576–85. http://dx.doi.org/10.1021/ef101125c.
[45] Gautam Kalghatgi, Algunaibet Ibrahim, Morganti Kai. On knock intensity and superknock in SI engines. SAE Int J Engines 2017;10(3):1051–63. http://dx.doi.org/10.4271/2017-01-0689.